

A digital prediction compensation for DR improvement in CT DSM with digital noise coupling

Jiaxi Pang,¹ Xilong Ou,¹ and Qiang Li¹

¹Institute of Integrated Circuits and Systems, University of Electronic Science and Technology of China, No.2006 Xiyuan Ave, Chengdu 611731, China

Email: qli@uestc.edu.cn

This paper presents a prediction-based dynamic range (DR) compensation technique in continuous-time (CT) delta -sigma modulator (DSM) with digital-domain noise coupling (DNC) structure. A digital prediction technique is proposed to address the issue of maximum stable amplitude (MSA) loss caused by DNC. The proposed prediction method has been shown to significantly extend the MSA of CT DSM with DNC. Moreover, through the extension of MSA, the DR and SNDR is significantly improved. A CTDSM with proposed compensation achieves a SNDR of 85.1dB at -1dBFS and a DR of 89dB.

Introduction: Analog-to-digital converter (ADC) with a high dynamic range (DR) is required in wireless communication systems. High order continuous-time (CT) delta-sigma modulators (DSMs) offer an excellent ADC solution for such scenarios with wide bandwidth (BW), owing to their decent power efficiency and inherent anti-aliasing feature. However, a higher order CT DSM suffers from high power consumption and stability issues in the single-loop topology[1, 2].

To address these challenges, noise coupling (NC) structures have been proposed to reduce the complexity of the loop filter[3]. However, a high order noise coupling filter implemented in the analog domain has several disadvantages such as hardware complexity, high power consumption and sensitivity to process-voltage-temperature (PVT) sensitivity. A digital domain filter was proposed to address the issues with the analog noise-coupling (ANC) structure. The digital noise-coupling (DNC) in [4, 5] eliminates the power-consuming analog circuits and realizes a simple noise-coupling filter in digital domain. In addition, the building blocks required for implementing the DNC structure can be implemented hardware efficiently by utilizing the structural advantages of the successive-approximation register (SAR) ADC.

However, since the quantization noise is directly injected into the input of quantizer (QTZ) in DNC structures, the maximum stable amplitude (MSA) of the modulator is reduced[6]. Although the degradation can be acceptable by choosing moderate QTZ resolution and DNC filter order, the MSA loss still limits the employment of high-order DNC structures in CT DSM, especially for applications that require high dynamic range.

To address the critical DR loss issue, a digital prediction compensation technique is proposed in this paper. Note that digital noise coupling structure is similar to mismatch error shaping (MES) which also suffers from loss of input range[7, 8]. By migrating input range compensation techniques which are widely used in MES technique, the DR of modulator can be significantly extended. Thus, the peak SNDR and dynamic range of CT DSM with DNC structure can be improved.

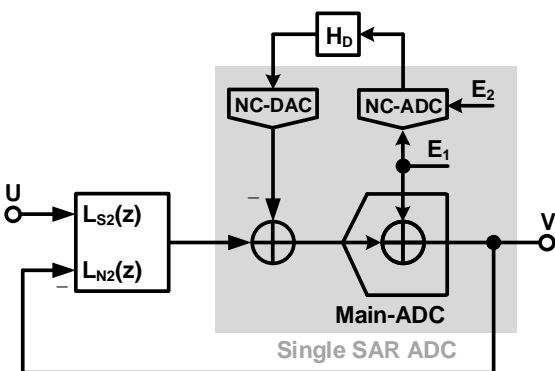


Fig 1 Block diagram of DNC.

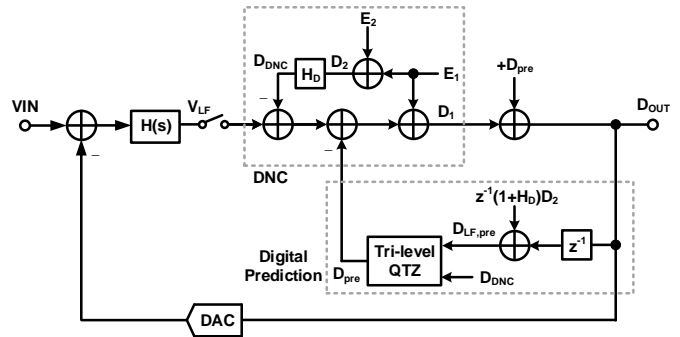


Fig 2 Block diagram of proposed digital prediction compensation in CT DSM with DNC.

Overview of DR loss in DNC: Fig 1 shows a simplified block diagram of the DNC structure in [4]. In this structure, the quantization noise E_1 is converted to digital code through the noise coupling ADC (NC-ADC) and then processed in the digital filter H_D . Then, the output of the digital filter is injected back to the input of the quantizer through the noise coupling digital-to-analog converter (NC-DAC), completing the loop for the digital noise-coupling. The circuit implementation of the digital filter consists only of registers and adder. Moreover, the main-ADC, NC-ADC, and NC-DAC are embedded in a single SAR ADC which makes the overall circuit implementation very efficient. The output of the DNC architecture is given by,

$$V = STF \cdot U + NTF(1 - H_D)E_1 - NTF \cdot H_D \cdot E_2 \quad (1)$$

where STF and NTF denote the signal transfer function (STF) and the noise transfer function (NTF) respectively. As shown in (1), E_1 is shaped by the DNC path as well as the main loop. For example, if the DNC filter H_D is set to $2z^{-1} - z^{-2}$, then $1 - H_D$ becomes a second-order high-pass filter which gives additional second-order noise-shaping to E_1 .

Note that, since the quantization noise E_1 is injected into the quantizer input, the MSA of the modulator is reduced [6]. For wide-band DSM designs, the loss of MSA can decrease the achievable DR which is much more unacceptable rather than the loss of SQNR. Although lower DNC filter order and higher main-ADC bit can improve MSA. However, lower DNC filter order reduces performance of noise shaping. Meanwhile, higher main-ADC bit increases requirements of feedback DAC linearity. Overall, the loss of MSA limits the SNDR and DR of DNC architecture and increases complexity of circuits.

Digital Prediction for DR Compensation: To address the issue of MSA loss, a compensation technique based on digital prediction is proposed. As shown in Fig 2, if V_{LF} and $-D_{DNC}$ have the same polarity, it can cause over range at input of quantizer which limits the MSA. The principle of proposed compensation is to generate a compensation voltage D_{pre} to shift the over-range input of quantizer back to the nominal conversion range. Meanwhile, to compensate for the additional voltage subtracted from the input of QTZ, the digital weight is added up to the digital output and fed to the feedback DAC. Thus, additional quantization levels are required in feedback DAC (FB DAC).

Fig.2 shows the implementation of the digital prediction compensation. As mentioned before, if polarity of V_{LF} and $-D_{DNC}$ can be detected, the proper compensation voltage D_{pre} would be generated and subtracted from input signal through the lowest-bit capacitor of MSB DAC. It is obvious that $-D_{DNC}$ can be directly obtained from the previous conversion results D_2 of NC-ADC. For example, if H_D is chosen to be $2z^{-1} - z^{-2}$, D_{DNC} is given by $D_{DNC}(n) = 2D_2(n - 1) - D_2(n - 2)$. However, V_{LF} is the loop-filter output of the present conversion cycle, and is unknown. To address this issue, digital prediction is used to generate an estimate of the V_{LF} . It should be noted that there exists correlation between $V_{LF}(n)$ and $V_{LF}(n - 1)$ due to oversampling, here $V_{LF}(n)$ is the discretization of the continuous-time output of loop-filter. Therefore, the digital quantization result of $V_{LF}(n - 1)$ which is denoted as $D_{LF}(n - 1)$ can be used to approximate $V_{LF}(n)$. The other hand, the main-ADC and NC-ADC are embedded in a single SAR ADC. The output of the single SAR ADC, $D_{OUT}(n) +$

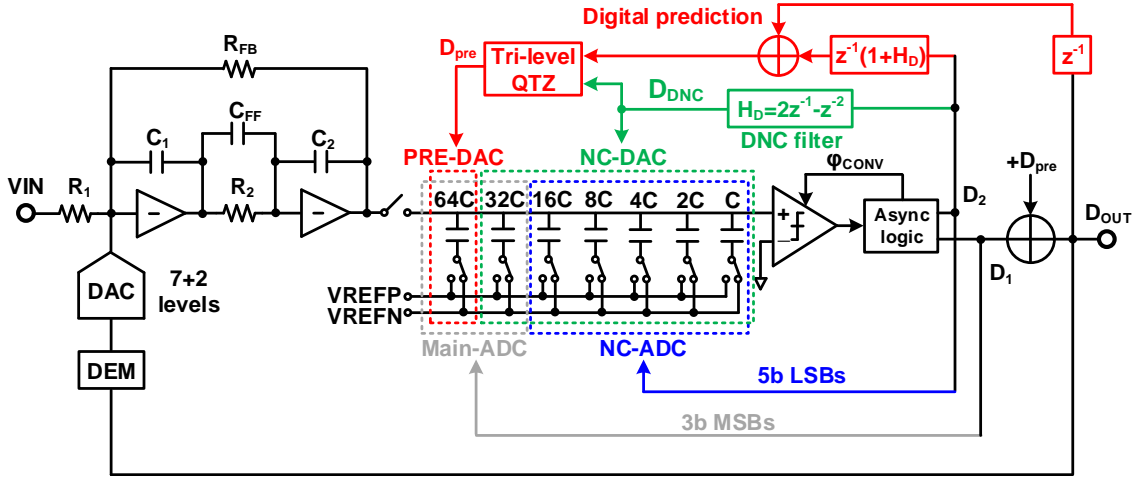


Fig 3 Implementation of proposed fourth-order CT DSM with second-order DNC and digital prediction compensation.

$D_2(n)$, can be used to denote the conversion results of input signal $V_{LF}(n) - D_{DNC}(n)$. Thus, the digital quantization result of $V_{LF}(n)$ is given by $D_{LF}(n) = D_{OUT}(n) + D_2(n) + D_{DNC}(n)$. Based on the above analysis, the digital prediction $D_{LF,pre}(n)$ for $V_{LF}(n)$ can be given by,

$$D_{LF,pre}(n) \approx D_{LF}(n-1) \\ = D_{OUT}(n-1) + (1+H_D)D_2(n-1) \quad (2)$$

Then, both the digital prediction of V_{LF} and $-D_{DNC}$ are generated by previous conversion codes. A tri-level QTZ is used to detected the polarity of $-D_{DNC}(n)$ and $D_{LF,pre}(n)$ and generate D_{pre} as follow,

$$D_{pre} = \begin{cases} \frac{2^{N+1}}{2^{M+N}} V_{REF}, & D_{LF,pre} > 0, -D_{DNC} > 0 \\ -\frac{2^{N+1}}{2^{M+N}} V_{REF}, & D_{LF,pre} < 0, -D_{DNC} < 0 \\ 0, & \text{others} \end{cases} \quad (3)$$

where the M and N denote the bits of prediction DAC (PRE-DAC) and NC-DAC respectively. Finally, to compensate for the additional D_{pre} subtracted from the input, the corresponding digital weight of D_{pre} is added up to the digital output which is fed to FB-DAC, which is given by $D_{OUT} = D_1 + D_{pre}$. Meanwhile, the additional levels in FB-DAC are also set to $2^{N+1}/2^{M+N} V_{REF}$. Thus, the signal to be quantized is recovered to the nominal range and the MSA is extended.

Implementation of CT DSM with DR Compensation: To verify the improvement of DR by using digital prediction compensation, a feed-forward (FF) CTDSM with DNC is adopted as shown in Fig 3. For an OSR of 16, the proposed CT DSM is clocked at 800 MHz for a 25-MHz bandwidth. The DNC filter is determined to be second order, and thus the loop filter is designed to be second order. As a result, fourth-order noise shaping is obtained. A 8-bit SAR ADC can work as a 3-bit main-ADC utilizing 2-bit MSB capacitors. The remaining 5-bit LSB capacitors are used for the 5-bit NC-ADC. In addition, the 6-bit LSB capacitors in the ADC are reused for the 6-bit NC-DAC. And the MSB capacitor is reused for the PRE-DAC. D_{pre} is predicted by the digital prediction path and injected back to the input of the QTZ through the PRE-DAC. The FB DAC is implemented with a current steering DAC architecture and DEM technique is used to improved its linearity.

Simulation results: Fig 4 illustrates the simulated SNDR versus input amplitude. As observed, the MSA at peak SNDR is -8dBFS for the 2nd-order DNC without compensation. After digital prediction compensation, the MSA at peak SNDR is extended to be -1dBFS. As depicted, the DR of modulator with compensation is 89dB, thus resulting in a significant improvement of 7dB over the modulator without MSA compensation. Meanwhile, the peak SNDR also has an 8dB improvement, from 77dB to 85dB. Fig 5 shows the simulated FFT spectrum. With a 2.44-MHz input signal, a peak SNDR of 85.1dB and SFDR of 100.4dB at -1dBFS are achieved.

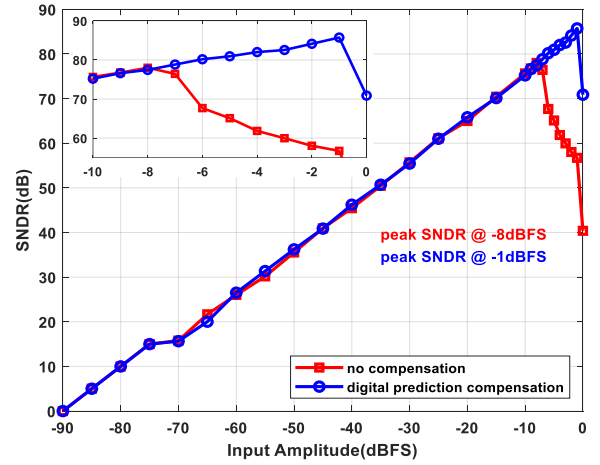


Fig 4 Simulated SNDR versus input amplitude

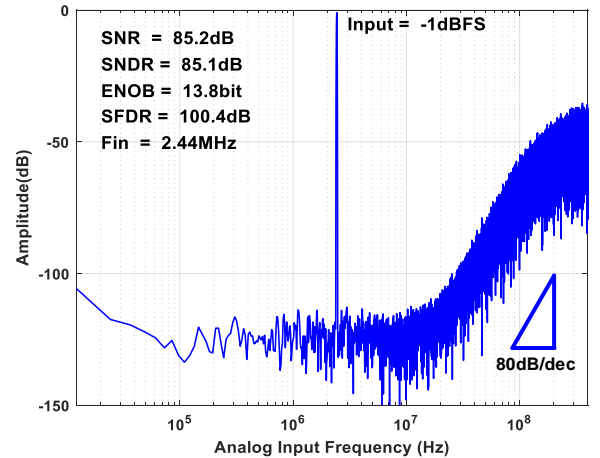


Fig 5 Simulated output spectrum with 2.44-MHz input frequency.

Conclusion: This paper presents an analysis of MSA loss which adversely impacts the achievable DR in CTDSM with DNC technique. Moreover, a digital prediction compensation is proposed to address the issue of MSA loss and improve the DR. The proposed digital prediction have been shown to significantly extend MSA and improve the DR. A CTDSM with digital prediction compensation achieves a SNDR of 85.1dB at -1dBFS. The proposed prediction-based compensation further expands the employment of DNC architecture in high-DR CT DSM design.

Acknowledgments: This work was supported by the National Natural Science Foundation of China under Grant 62090041 and Grant NSFC-DFG-61761136015.

© 2023 The Authors. *Electronics Letters* published by John Wiley & Sons Ltd on behalf of The Institution of Engineering and Technology

This is an open access article under the terms of the Creative Commons Attribution License, which permits use, distribution and reproduction in any medium, provided the original work is properly cited.

Received: 10 January 2021 Accepted: 4 March 2021

doi: 10.1049/ell2.10001

References

1. Qi, L., et al.: Wideband Continuous-Time MASH Delta-Sigma Modulators: A Tutorial Review. *IEEE Transactions on Circuits and Systems II: Express Briefs* 69(6), 2623–2628 (2022). doi:10.1109/TCSII.2022.3163766
2. Ortmanns, M.: Wideband and low-power delta-sigma adcs: State of the art, trends and implementation examples. In: ESSCIRC 2021 - IEEE 47th European Solid State Circuits Conference (ESSCIRC), , pp. 28–35. (2021)
3. Lee, K., Miller, M.R., Temes, G.C.: An 8.1 mW, 82 dB Delta-Sigma ADC With 1.9 MHz BW and -98 dB THD. *IEEE Journal of Solid-State Circuits* 44(8), 2202–2211 (2009). doi:10.1109/JSSC.2009.2022298
4. Jang, I.H., et al.: A 4.2-mW 10-MHz BW 74.4-dB SNDR Continuous-Time Delta-Sigma Modulator With SAR-Assisted Digital-Domain Noise Coupling. *IEEE Journal of Solid-State Circuits* 53(4), 1139–1148 (2018). doi:10.1109/JSSC.2017.2778284
5. Rezapour, A., Shamsi, H.: Digital noise coupled mesh delta-sigma modulator. *IEEE Transactions on Circuits and Systems II: Express Briefs* 66(1), 41–45 (2019). doi:10.1109/TCSII.2018.2837123
6. Wu, B., et al.: A 24.7 mW 65 nm CMOS SAR-Assisted CT $\Delta\Sigma$ Modulator With Second-Order Noise Coupling Achieving 45 MHz Bandwidth and 75.3 dB SNDR. *IEEE Journal of Solid-State Circuits* 51(12), 2893–2905 (2016). doi:10.1109/JSSC.2016.2594953
7. Shen, Y., et al.: A 103-dB SFDR Calibration-Free Oversampled SAR ADC With Mismatch Error Shaping and Pre-Comparison Techniques. *IEEE Journal of Solid-State Circuits* 57(3), 734–744 (2022). doi:10.1109/JSSC.2021.3135559
8. Liu, J., et al.: Error-Feedback Mismatch Error Shaping for High-Resolution Data Converters. *IEEE Transactions on Circuits and Systems I: Regular Papers* 66(4), 1342–1354 (2019). doi:10.1109/TCSI.2018.2879582

Please ensure that your Letter does not exceed the maximum length of 6 columns/3 pages.